Applications of Interval Algorithms in Engineering

Eberhard P. Hofer and Andreas Rauh
Institute of Measurement, Control, and Microtechnology
University of Ulm
D-89069 Ulm, Germany
{EP.Hofer, Andreas.Rauh}@uni-ulm.de

Abstract

The optimization of the functionality and the guarantee of a safe operation of a technical system are important issues in industry. These aspects become even more important when we have to deal with numerous uncertainties which heavily influence the behavior of the technical system under consideration and — in the worst case — cause system failure. Appropriate interval tools can offer solutions to problems where system uncertainties play a key role. Over the recent years at the Institute of Measurement, Control, and Microtechnology existing interval tools have been extended and new modules have been developed.

In this contribution, successful applications of interval algorithms to real-world problems in various fields of engineering are presented. The focus is on measuring techniques including interval observers and sensitivity analysis as well as design of optimal and robust controllers for continuous-time and discrete-time systems.

1 Introduction

In this paper, an overview of various applications of interval algorithms in engineering is given[1]. A common basis of all applications is a given mathematical model of the relevant technical system described by sets of algebraic equations and ordinary differential equations. In general, two different types of problems can be considered which are steady state analysis and analysis of the transient behavior of a dynamical system.

For most practically relevant dynamical systems, guaranteed knowledge about the influence of uncertainties of both initial states and system parameters is of importance. In the following, different applications are presented in order to highlight the benefits of the use of interval methods [8, 13].

[1]For a complete list of recent applications of interval methods investigated by the authors, the reader is referred to `http://www.interval-methods.de`.

An application in automotive engineering covers the influence of unavoidable manufacturing errors on the functionality of a mechanical component. As a result, quality control in production can be improved. A further application deals with guaranteed estimation of physical parameters for characterization and model validation of a micro-electromechanical device.

Safety-critical applications in X-by-wire systems, e.g., automobiles and aircrafts, influenced by sensor uncertainties usually require the verification of the systems' functionality. Such uncertainties may not only affect the behavior of the feedback control, but also the monitoring of the function in the control unit and, thus, may lead to delayed or even false reactions in case of failure. Therefore, it is extremely important to get reliable results about the influence of sensor tolerances on the dynamic behavior of the closed-loop system. The task is formulated as a global interval optimization problem. It is solved by using advanced interval algorithms keeping all safety-critical states within a pre-defined limit.

In addition to safety aspects, reduction of operation costs of a plant is always a strong issue. In an application taken from environmental engineering the efficiency of interval methods not only for reliable plant operation but also for plant and controller design is shown.

Section 2 summarizes the notation used in this paper for the description of technical systems with uncertainties. The selected applications in engineering can be associated with the following problems:

- **Steady state analysis for time-invariant systems (Sec. 3).** The applications are a rocker arm (Sec. 3.1) and a micro relay (Sec. 3.2).
- **Analysis of *discrete*-time dynamical systems with time-*invariant* parameter uncertainties (Sec. 4).** The applications are an airbus elevator (Sec. 4.1) and a common-rail injection (Sec. 4.2).
- **Analysis of *continuous*-time dynamical systems with time-*varying* parameter uncertainties (Sec. 5).**

The application is a subsystem of biological wastewater treatment processes (Sec. 5.2).

- **State and parameter estimation using interval observers (Sec. 6).** The applications are an electrostatic microactuator (Sec. 6.1) and a micropositioning system (Sec. 6.2).

Section 7 summarizes the most important benefits that have been achieved by the use of interval methods for the applications presented here. An outlook on future research concludes this contribution.

2 Technical Systems with Uncertainties

The technical applications considered in this paper are described both by the discrete-time state-space representation

$$\begin{bmatrix} x_{k+1} \\ p_{k+1} \end{bmatrix} = \begin{bmatrix} g_k\left(x_k, p_k, u_k, k\right) \\ g_{p,k}\left(p_k, \Delta p_k\right) \end{bmatrix} \tag{1}$$

and — in the case of continuous-time processes — by ordinary differential equations

$$\begin{bmatrix} \dot{x}\left(t\right) \\ \dot{p}\left(t\right) \end{bmatrix} = \begin{bmatrix} f\left(x\left(t\right), p\left(t\right), u\left(t\right), t\right) \\ \Delta p\left(t\right) \end{bmatrix} \quad . \tag{2}$$

In both cases, uncertainties of the initial conditions of the state vector x have to be taken into account. For discrete-time models they are denoted by $x_0 \in [x_0] := [\underline{x}_0 \; ; \; \overline{x}_0]$, for continuous-time systems by $x\left(0\right) \in [x\left(0\right)] := [\underline{x}\left(0\right) \; ; \; \overline{x}\left(0\right)]$. In both system models, control vectors are denoted by u. All uncertain system parameters are represented by the parameter vector p which is bounded by the intervals $p_k \in \left[\underline{p}_k \; ; \; \overline{p}_k\right]$ for all $k \geq 0$ and $p\left(t\right) \in \left[\underline{p}\left(t\right) \; ; \; \overline{p}\left(t\right)\right]$ for all $t \geq 0$, respectively.

For time-varying parameter uncertainties, their variation rates Δp are not vanishing. Uncertainties of these quantities can be modeled by the intervals $\Delta p_k \in \left[\underline{\Delta p}_k \; ; \; \overline{\Delta p}_k\right]$ and $\Delta p\left(t\right) \in \left[\underline{\Delta p}\left(t\right) \; ; \; \overline{\Delta p}\left(t\right)\right]$, respectively. In Fig. 1, the influence of non-vanishing parameter variation rates Δp is depicted for the scalar case.

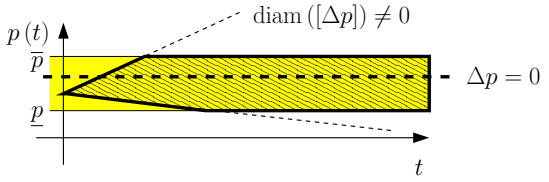

Figure 1. Time behavior of time-varying parameter uncertainties.

3 Steady State Analysis for Time-Invariant Systems

In order to analyze the steady state of a discrete-time dynamical system, the algebraic equations

$$x = g\left(x, p, u\right) \tag{3}$$

have to be solved. In the continuous-time case, the steady state is determined by solving the nonlinear algebraic equations

$$0 = f\left(x, p, u\right) \quad . \tag{4}$$

In both scenarios, interval enclosures for all physically relevant solutions $x = x\left(p, u\right)$ with $p \in [p]$ have to be determined. To deal with this problem, possible interval arithmetic approaches are:

Solution Approach 1
(i) Subdivision of the physically relevant domain $[x]$.
(ii) Consistency tests for all subintervals of $[x]$ by interval evaluation of g and f in (3) and (4).

Solution Approach 2
(i) Subdivision of physically relevant domain $[x]$ (*optional*).
(ii) Application of interval Newton methods, e.g. Krawczyk operator.

3.1 Rocker Arm

As a first application in steady state analysis of nonlinear systems with uncertainties, the tolerances of motion of the valve lifter depicted in Fig. 2 are determined for the known uncertain system parameters p_i, $i = 1, \ldots, 8$,

$$\begin{aligned} p_1 &:= R_G \;\; \in [16 \; ; \; 16.01] \\ p_2 &:= R_S \;\; \in [25 \; ; \; 25.01] \\ p_3 &:= Dist \in [42 \; ; \; 42.01] \\ p_4 &:= L_1 \;\; \in [27.5 \; ; \; 27.501] \\ p_5 &:= \Delta\epsilon \;\; \in [0.7 \; ; \; 0.7] \\ p_6 &:= K_2 \;\; \in [4 \; ; \; 4.001] \\ p_7 &:= L_4 \;\; \in [34 \; ; \; 34.01] \\ p_8 &:= R_1 \;\; \in [10 \; ; \; 10.001] \quad . \end{aligned} \tag{5}$$

The motion of the considered valve lifter is described by

$$\begin{aligned} x_1 := S_V(p_i) &= p_8 \; + \; p_6 \; - \; p_7 \cos\delta(p_i) \\ x_2 := V_V(p_i) &= p_7 H_4(p_i) \sin\delta(p_i) \\ x_3 := B_V(p_i) &= p_7 \cdot [H_4^2(p_i) \cos\delta(p_i) \\ &\quad + H_6(p_i) \sin\delta(p_i)] \quad , \end{aligned} \tag{6}$$

where the functions H_4, H_6, and δ are explicitly given by the geometry of the system, see [22]. In equation (6), the variable S_V denotes the position of the valve lifter, V_V its velocity, and B_V its acceleration.

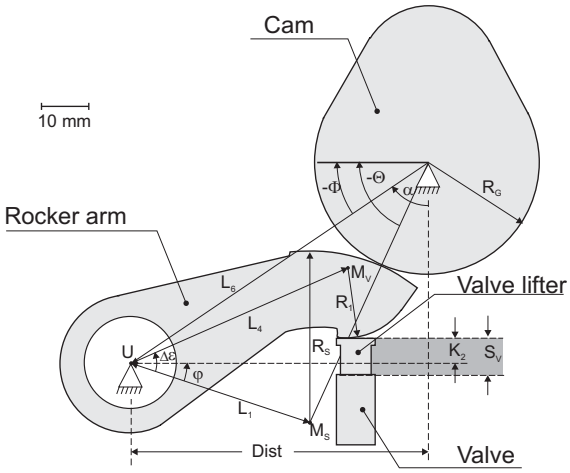

Figure 2. System parameters of a rocker arm.

The goal of the steady state analysis for this system is to determine guaranteed bounds for all variables x_j, $j = 1, 2, 3$ according to

$$\begin{aligned} x_1 \in [\underline{x}_1\,;\,\overline{x}_1] &= [\min S_V(p_i)\,;\max S_V(p_i)] \\ x_2 \in [\underline{x}_2\,;\,\overline{x}_2] &= [\min V_V(p_i)\,;\max V_V(p_i)] \\ x_3 \in [\underline{x}_3\,;\,\overline{x}_3] &= [\min B_V(p_i)\,;\max B_V(p_i)]\ . \end{aligned} \tag{7}$$

In the following, the results obtained by natural interval arithmetic, mean-value rule evaluation, and optimized interval arithmetic based on global optimization [3] including mean-value rule evaluation and monotonicity tests are summarized.

Natural interval evaluation

$$\begin{aligned} S_V(\Phi) &= [2.23940; 2.35208] \\ V_V(\Phi) &= [2.04417; 2.61488] \\ B_V(\Phi) &= [-6.23038; 10.29386] \end{aligned} \tag{8}$$

Mean-value rule evaluation

$$\begin{aligned} S_V(\Phi) &= [2.29515; 2.29634] \\ V_V(\Phi) &= [2.32611; 2.32874] \\ B_V(\Phi) &= [2.35106; 2.41480] \end{aligned} \tag{9}$$

For the optimized interval evaluation the following outer interval enclosures and inner interval enclosures have been determined:

Outer interval enclosures in optimized evaluation

$$\begin{aligned} S_V(\Phi) &= [\underline{2.295}244; \underline{2.296}247] \\ V_V(\Phi) &= [\underline{2.326}920; \underline{2.327}928] \\ B_V(\Phi) &= [\underline{2.382}394; \underline{2.383}468] \end{aligned} \tag{10}$$

Inner interval enclosures in optimized evaluation

$$\begin{aligned} S_V(\Phi) &= [\underline{2.295}318; \underline{2.296}160] \\ V_V(\Phi) &= [\underline{2.327}011; \underline{2.327}837] \\ B_V(\Phi) &= [\underline{2.382}495; \underline{2.383}367] \end{aligned} \tag{11}$$

The desired accuracy between the outer and inner interval bounds has been chosen as $\epsilon = 10^{-4}$ for each x_j. As displayed in the sketch in Fig. 3, the inner interval enclosures are always completely included in the outer ones. By the outer and inner interval bounds (10) and (11), an enclosure of the *true range* of the variable x_j is given. For the sake of comparison with non-validated evaluation techniques, the range of all x_j has been approximated by a Monte-Carlo simulation [2] using 10,000 samples. The resulting bounds are given in (12) and Fig. 4.

Monte-Carlo simulation

$$\begin{aligned} S_V(\Phi) &= [2.29529; 2.29621] \\ V_V(\Phi) &= [2.32797; 2.32789] \\ B_V(\Phi) &= [2.38248; 2.38339] \end{aligned} \tag{12}$$

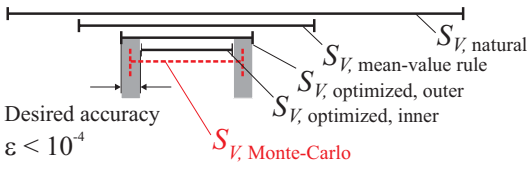

Figure 3. Reduction of overestimation by sophisticated interval techniques for range computation.

It should be pointed out that Monte-Carlo methods — especially for complex, higher-dimensional systems — can only provide tight bounds for the desired range if huge numbers of sampling points are used. Hence, it cannot be guaranteed that the bounds computed by Monte-Carlo simulations are contained within the inner and outer enclosures determined using interval arithmetic.

3.2 Micro Relay

As a second application, the estimation of system parameters for the micro relay displayed in Fig. 5 is considered [6]. Based on rough a priori enclosures of the range

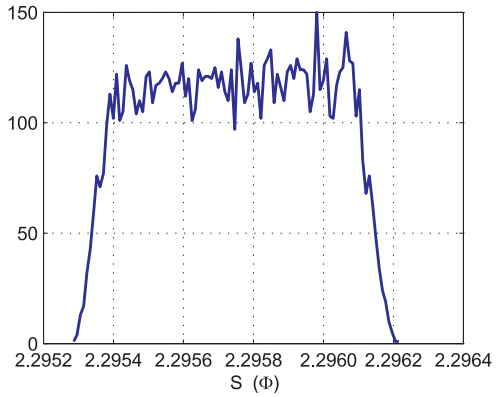

Figure 4. Monte-Carlo simulation as reference for the quality of the computed interval bounds of S_V.

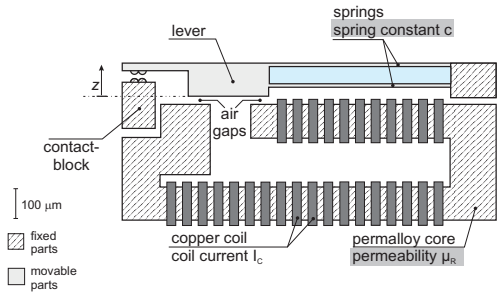

Figure 5. Micro relay.

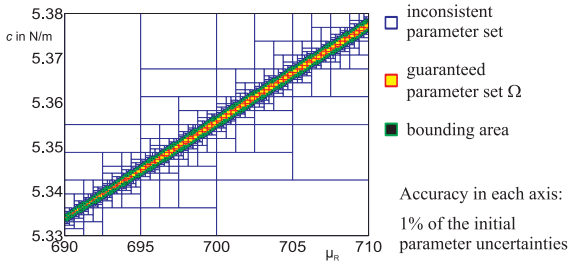

Figure 6. Consistent and inconsistent parameter sets for the micro relay within the a priori enclosures.

of the spring constant $c \in [5.33; 5.38]\,\mathrm{N/m}$ and the permeability $\mu_R \in [690; 710]$ of the permalloy core as well as uncertain measurements of the displacement z of the lever, the parameter estimates have to be improved such that only values are obtained which are consistent with all measured data. The measurement of the displacement has been carried out 23 times for various coil currents I_c with an uncertainty of $\pm 0.3\mu\mathrm{m}$ of the measured position. Using the measurement equations

$$\begin{aligned} z_j(\mu_R, c) &= \frac{2\gamma(\mu_R)}{3} \\ &\quad \cdot \left(\cos\left(\frac{1}{3} \arccos\left(1 - \frac{27\vartheta(c, I_{cj})}{2\gamma(\mu_R)^3} \right) \right) - 1 \right) \\ \gamma(\mu_R) &= \frac{L_{Fe} A_G}{2\mu_R A_{Fe}} + \delta_0 \\ \vartheta(c, I_{cj}) &= \frac{N^2 A_G \mu_0 I_{cj}^2}{4c}\,, \quad j = 1, \ldots, 23 \end{aligned} \tag{13}$$

the admissible set Ω of the spring constant c and the permeability μ_R is given by

$$\Omega = \left\{ \begin{bmatrix} \mu_R \\ c \end{bmatrix} \middle| \begin{array}{r} |\hat{z}_j(I_{cj}) - z(\mu_R, c)| \leq 0.3\mu\mathrm{m}, \\ j = 1, \ldots, 23 \end{array} \right\} . \tag{14}$$

The resulting guaranteed parameter set Ω and the bounding area containing the intervals which separate the consistent and inconsistent parameter values are depicted in Fig. 6. The accuracy of the computed sets can be influenced by specification of the maximum admissible width of each component of the undecided intervals. Here, an accuracy of 1% of the initial parameter uncertainties has been specified.

4 Discrete-Time Dynamical Systems with Time-Invariant Parameter Uncertainties

After the discussion of techniques and applications of steady state analysis of dynamical systems with uncertainties, the *dynamics* of discrete-time models and continuous-time models is analyzed in Sections 4 and 5, respectively.

According to Section 2, a discrete-time system is given by the state-space representation

$$\begin{bmatrix} x_{k+1} \\ p_{k+1} \end{bmatrix} = \begin{bmatrix} g_k\left(x_k, p_k, u_k, k\right) \\ g_{p,k}\left(p_k, \Delta p_k\right) \end{bmatrix} . \tag{15}$$

For time-invariant uncertainties, the relations $\Delta p_k = 0$ and $p_{k+1} = p_k$ hold for all $k \geq 0$. For the following analysis it is assumed that u_k is either a given open-loop or closed-loop control law. Using interval arithmetic evaluation of the mathematical system models for all uncertain parameters, guaranteed state enclosures have to be determined for each time step k for a given finite time horizon. In the following list of possible solution approaches, only those are

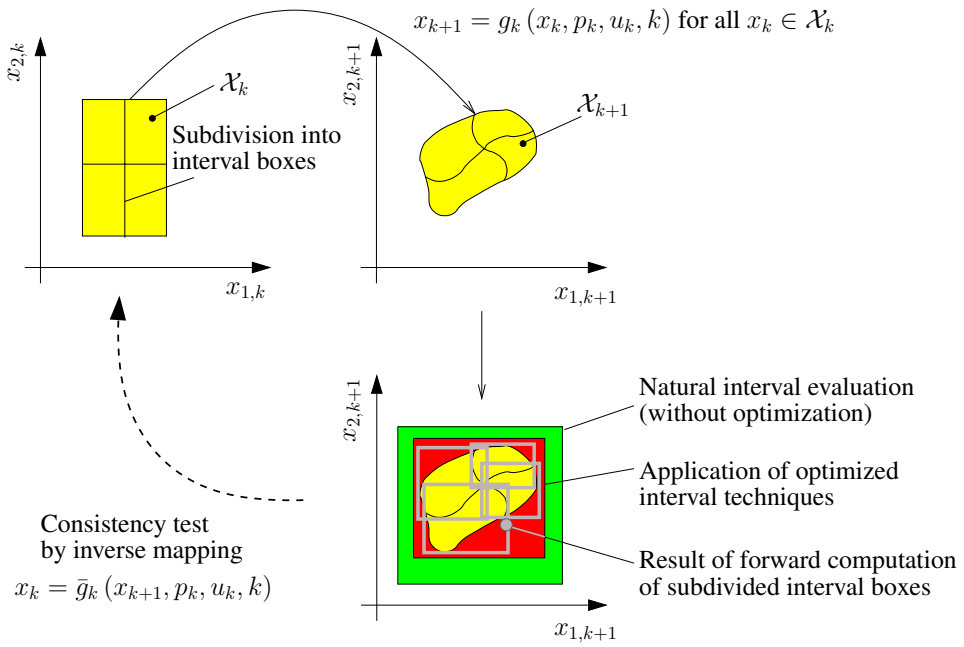

Figure 7. Interval arithmetic simulation of dynamical processes with subdivision into interval boxes, propagation of subintervals, and consistency tests.

mentioned which have been used in the selected applications [4].

Solution Approach 1. The basic approach for calculation of guaranteed state enclosures of discrete-time systems is the recursive computation of the state intervals

$$[x_{k+1}] = g_k\big([x_k]\,,[p_k]\,,u_k,k\big) \tag{16}$$

for open-loop control and

$$[x_{k+1}] = g_k\big([x_k]\,,[p_k]\,,u_k\,([x_k])\,,k\big) \tag{17}$$

in the case of closed-loop control.

Solution Approach 2. To reduce overestimation caused by the wrapping effect, computation of the state enclosures $[x_{k+1}]$ can be improved by coordinate transformations. The simplest possibility is a linear transformation according to

$$\begin{aligned} [x_k] &= T_k \cdot [\tilde{x}_k] \\ [\tilde{x}_{k+1}] &= T_{k+1}^{-1} \cdot g_k\big(T_k \cdot [\tilde{x}_k]\,,\big[p_k\big],u_k,k\big) \quad . \end{aligned} \tag{18}$$

Solution Approach 3. In Fig. 7, subdivision of state intervals $[x_{k+1}]$ is used for the computation of tight enclosures of complexly shaped regions if the coordinate transformation in the *Solution Approach 2* does not result in the desired quality.
(i) Consistency tests by inverse mapping of the state equation according to

$$[x_k] = \bar{g}_k\big([x_{k+1}]\,,[p_k]\,,u_k,k\big) \quad , \tag{19}$$

where the interval $[x_{k+1}]$ denotes the subintervals obtained by forward computation [10].
(ii) Interval Newton methods for state equations where the inverse mapping cannot be calculated analytically.
(iii) Merging of subintervals in case of small overestimation of the union of the merged subintervals is described in detail in [19].

Solution Approach 4. Computation of state variables $[x_{k+1}]$ by explicit replacement of $[x_k]$, $[x_{k-1}]$, …, $[x_2]$, $[x_1]$ in terms of the initial state $[x_0]$ and all parameter uncertainties $[p_0]$, $[p_1]$, …, $[p_{k-1}]$, $[p_k]$, i.e.,

$$\begin{aligned} [x_{k+1}] = g_k\Bigg(g_{k-1}\Big(\,\dots \\ g_1\Big(g_0\,([x_0]\,,[p_0]\,,u_0,0)\,,[p_1]\,,u_1,1\Big)\,\dots\Big)\Bigg) \quad . \end{aligned} \tag{20}$$

Here, mean-value rule evaluation, monotonicity tests, and global optimization techniques are useful approaches to significantly reduce overestimation caused by multiple dependency of the state equation (15) upon the components of the interval vectors $[x_k]$ and $[p_k]$.

4.1 Airbus Elevator

For the elevator control loop depicted in Fig. 8, interval enclosures for the actual elevator angle δ and the servo valve position x_V are of interest for a given time horizon [5].

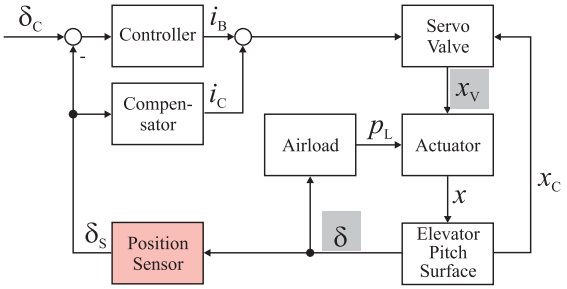

Figure 8. Airbus elevator.

This dynamical system can be modeled with sufficient accuracy by the discrete-time equations

$$
\begin{aligned}
x_{k+1} &= x_k + \sqrt{5}\cdot 10^5 \frac{B}{A} x_v h \Delta t,\\
y_k &= \delta = k_{SPAP}\, x_k,\\
h &= \boxed{\operatorname{sign}(z)\,\sqrt{|z|}},\\
z &= \left(\frac{2}{1+\frac{k^*_{MQ} B^2 x_V^2}{2\,A^2}} - 1 \right) (\Delta p_s - p_L \boxed{\operatorname{sign}(x_V)}),\\
p_L &= -\frac{100}{A}(a + b\,\delta)\, c\, v_{CAS}^2, \qquad (21)\\
x_V &= k_{SV}\, k_{SC}(i_C + i_B) - x_C,\\
x_C &= k_{Fb}\, k_C\, x,\\
i_B &= k_R\,(\delta_C - \delta_S),\\
i_C &= k_{Cp}\,\delta_S,\\
\delta_S &= r\,\delta + \delta_{offs}\ ,
\end{aligned}
$$

where the reference elevator angle is denoted by δ_C, the measured elevator angle by δ_S, the control output by i_B, the compensating current by i_C, the load pressure by p_L the hydraulic cylinder position by x, and the mechanical feedback by x_C. The functions highlighted by gray boxes in (21) are not continuously differentiable. The uncertainties of the position sensor in the closed-loop control are

$$r = [0.98\ ;\ 1.02] \quad \text{and} \quad \delta_{offs} = [-0.6\ ;\ 0.6]\ . \qquad (22)$$

For the desired accuracies $\epsilon_\delta = 0.1^\circ$ of the actual elevator angle δ and $\epsilon_x = 0.01\text{mm}$ of the servo valve position x_V, interval enclosures of their time responses are shown in Figs. 9 and 10, respectively.

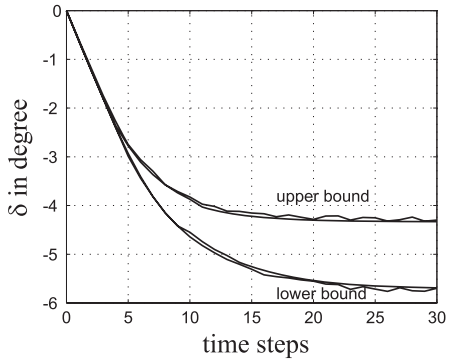

Figure 9. Interval bounds for the time response of the actual elevator angle δ.

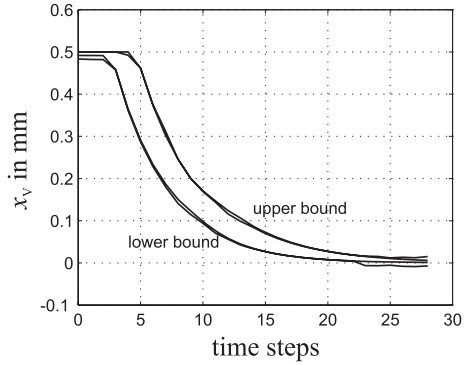

Figure 10. Interval bounds for the time response of the servo valve position x_V.

4.2 Common-Rail Injection System

Analogously to the previous application, the sensitivity of the closed-loop control of the common-rail injection system in Fig. 11 is analyzed [21]. This system is described by the discrete-time model given by the equations (23)–(26). The reference pressure is denoted by p_{ref}, the drive voltage by u, the tappet displacement by x_c, and the measured rail pressure by p_{sensor}.

Mathematical model of the common-rail injection system

Common-rail injection

$$
\begin{aligned}
p_{rail,k+1} &= f_{lim,p}\left(p_{rail,k} + \frac{q_{pump} - q_{ab1} - q_{ab2}}{V\,\kappa}\,\Delta t\right) \\
q_{ab1} &= A_{flow}\alpha_{furb}\sqrt{\frac{p_{rail,k} - p_{ab}}{5\,\rho}}, \quad \rho = \frac{824 - 0.68\,(t_\rho - 15)}{1 - \frac{0.06\,p_{rail,k}}{639\ + p_{rail,k}}} \\
A_{flow} &= \min\left(\frac{\pi}{2}\,x_{C,k}\left(d + \frac{x_{C,k}}{\sqrt{2}}\right),\ \frac{\pi}{16}\,d^2\right)
\end{aligned}
\tag{23}
$$

Magnetic valve

$$
\begin{aligned}
x_{C,k+1} &= f_{lim,x}(x_{C,k} + (F_{err} - c\,x_{C,k})\,\Delta t), \quad F_{err} = F_{hyd} - F_0 - F_{mag} \\
F_{mag} &= k_1\left(\omega\frac{f_{lim,z}\left(1 - \mathrm{e}^{-\frac{i_{L,k}}{k_3}}\right)}{f_{lim,n}(k_2 + 0.001\,x_{C,k})}\right)^2 \\
F_{hyd} &= k_0\,\frac{p_{rail,k} - p_{ab} + k_1\,x_{C,k}}{k_2 + x_{C,k}} \\
i_{L,k+1} &= i_{L,k} + \frac{u_{in} - R\,i_{L,k}}{L}\Delta t, \quad u_{in} = u_{batt}\,f_{lim,u}(u)
\end{aligned}
\tag{24}
$$

Controller

$$
\begin{aligned}
u &= f_{stat}(p_{ref}) + u_P + u_{I,k} + u_D \\
u_p &= K_R\,e_k, \quad e_k = p_{ref} - p_{sensor} \\
u_{I,k+1} &= u_{I,k} + e_k\,\frac{K_R}{T_I}\,f_{switch}(u_P, u_D) \\
u_D &= K_R T_D\,\frac{e_k - e_{k-1}}{\Delta t}
\end{aligned}
\tag{25}
$$

Sensor characteristic

$$
p_{sensor} = r\,p_{rail,k} + p_{offs} \tag{26}
$$

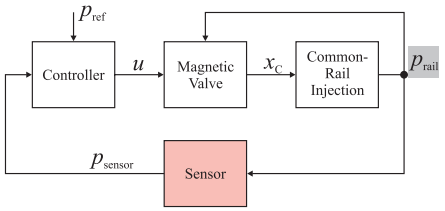

Figure 11. Common-rail injection system.

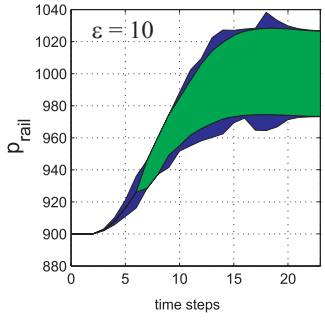

Figure 12. Inner and outer interval enclosures for the rail pressure p_{rail}.

The functions highlighted by gray boxes in (23)–(26) contain system-dependent static nonlinearities as well as saturation and switching characteristics which are not continuously differentiable. Hence, special treatment of these terms is necessary for the application of evaluation techniques which use partial derivatives of the state equations w.r.t. parameters and states. These are, for example, evaluation techniques aiming at the reduction of overestimation such as mean-value rule evaluation and monotonicity tests which are summarized in [4]. In the sensitivity analysis, the uncertainty $r \in [0.97\ ;\ 1.03]$ of the parameter of the pressure sensor is considered. The resulting interval enclosures for the actual rail pressure p_{rail} are shown in Fig. 12. The desired accuracy of the actual rail pressure p_{rail} in the global optimization approach used for computation of inner and outer interval bounds has been set to $\epsilon = 10$.

5 Continuous-Time Dynamical Systems with Time-Varying Parameter Uncertainties

5.1 Theoretical Background

In addition to discrete-time processes which have been discussed in the previous Section, continuous-time systems

described by sets of ordinary differential equations ODEs are widely used system representations in engineering. The considered ODEs are assumed to be given in state-space representation according to

$$\begin{bmatrix} \dot{x}_s(t) \\ \dot{p}(t) \end{bmatrix} = \begin{bmatrix} f_s(x_s(t), p(t), u(t), t) \\ \Delta p(t) \end{bmatrix} , \quad (27)$$

where the system parameters are time-varying, i.e., $\Delta p(t) \neq 0$ and $\mathrm{diam}([\Delta p]) \neq 0$ usually hold for all $t \geq 0$. For given bounded uncertainties of the initial state vector, given bounded parameter uncertainties, and given open-loop and closed-loop control laws $u(t)$ and $u(x(t))$, guaranteed state enclosures have to be determined at each point of time t for a given finite time horizon.

To simplify the notation for the solution approaches discussed in the following, the extended state vector

$$x(t) := \left[x_s^T(t) \quad p^T(t)\right]^T \quad (28)$$

is introduced. This allows to rewrite the state equations (27) in the form

$$f(\cdot) := \begin{bmatrix} f_s(x(t), u(t), t) \\ \Delta p(t) \end{bmatrix} . \quad (29)$$

Solution Approach 1. The computation of state enclosures of an initial value problem IVP by series expansion *with respect to time* according to

$$[x(t_{k+1})] = [x(t_k)] + h_k \cdot \phi([x(t_k)], u_k, t_k) + [e_k] \quad (30)$$

with

$$\phi(\cdot) := \sum_{i=1}^{\nu} \frac{h_k^{i-1}}{i!} \cdot \frac{d^{i-1} f(\cdot)}{dt^{i-1}} \quad (31)$$

and the discretization error interval

$$[e_k] := \left. \frac{h_k^{\nu+1}}{(\nu+1)!} \cdot \frac{d^{\nu} f(\cdot)}{dt^{\nu}} \right|_{[\tau_k],[B_k]} \quad (32)$$

is the basis for several validated ODE solvers such as VNODE by Nedialkov [14]. Here, the bounds for the discretization error have to be evaluated for a bounding box of all states and parameters $[B_k]$ which can be reached in the time interval $[\tau_k] := [t_k \ ; \ t_{k+1}]$. This bounding box is usually either determined with the help of the Picard iteration or with the help of higher order enclosure methods [15].

Solution Approach 2. Furthermore, state enclosures of IVPs can also be computed by series expansions with respect to time *and initial states*. This approach is implemented in the Taylor-model-based solver COSY VI by Berz and Makino [12].

Solution Approach 3. A novel approach for the computation of state enclosures $[x_{encl}(t)] := x_{app}(t) + [R(t)]$ of IVPs — not based on series expansions — relies on non-validated approximate solutions $x_{app}(t)$ and guaranteed error bounds $[R(t)]$. This technique is implemented in VALENCIA-IVP by Rauh and Auer [1].

5.2 Biological Wastewater Treatment

The dynamical behavior of biological wastewater treatment plants has to be robust w.r.t. changes of most system parameters [10, 19]. Furthermore, cost-effective plant operation demands for a reduction of the oxygen input rate into the aeration tank to its lowest possible value. Hence, it is necessary to find a suitable compromise between both prerequisites. To deal with this problem, interval arithmetic simulation of mathematical system models such as the Activated Sludge Model No. 1 ASM1 of the International Water Association, under consideration of time-varying uncertain system parameters, is a useful technique. In the following, the *Solution Approach 1* using a validated explicit Euler method with subdividing and merging of interval boxes is applied to simulation of a subsystem model of a wastewater treatment plant as shown in Fig. 13.

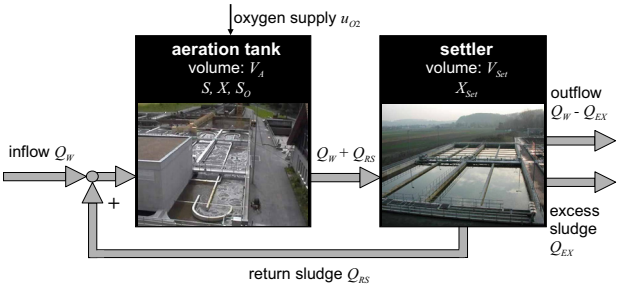

Figure 13. Biological wastewater treatment plant.

The state equations

$$\begin{aligned} \dot{S} =& \frac{Q_W}{V_A}(S_W - S) - \mu(S, S_O)\frac{1}{Y}X \\ \dot{X} =& -\frac{Q_W}{V_A}X + \frac{Q_{RS}}{V_A}(X_{Set} - X) \\ & + (\mu(S, S_O) - b)X \\ \dot{S}_O =& \frac{Q_W}{V_A}(S_{OW} - S_O) - \mu(S, S_O)\frac{1-Y}{Y}X \\ & + \frac{\rho_{O2}}{V_A}\left(1 - \frac{S_O}{S_{O,sat}}\right)u_{O2} \\ \dot{X}_{Set} =& \frac{Q_W + Q_{RS}}{V_{Set}}X - \frac{Q_{EX} + Q_{RS}}{V_{Set}}X_{Set} , \end{aligned} \quad (33)$$

where the nonlinear growth rate of substrate consuming bacteria is modeled by the Monod kinetics

$$\mu(S, S_O) = \hat{\mu}_H \frac{S}{S + K_S}\frac{S_O}{S_O + K_{OS}} , \quad (34)$$

describe the reduction of biodegradable organic substrate by heterotrophic bacteria. The state variables are the con-

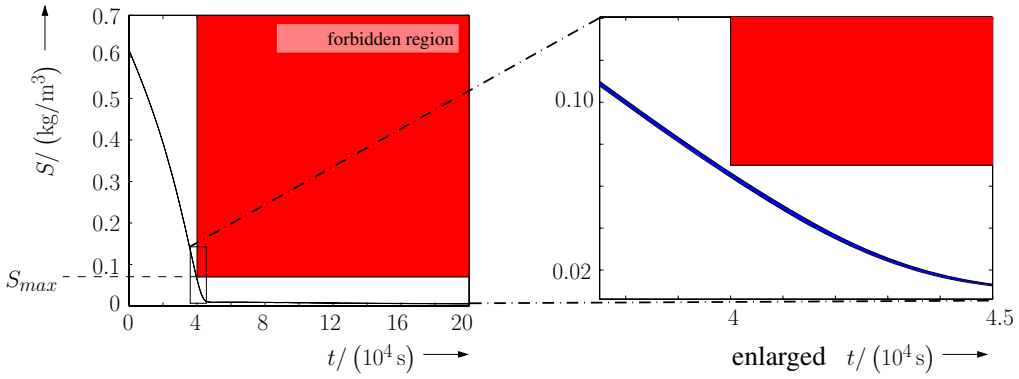

Figure 14. Substrate concentration S in the aeration tank.

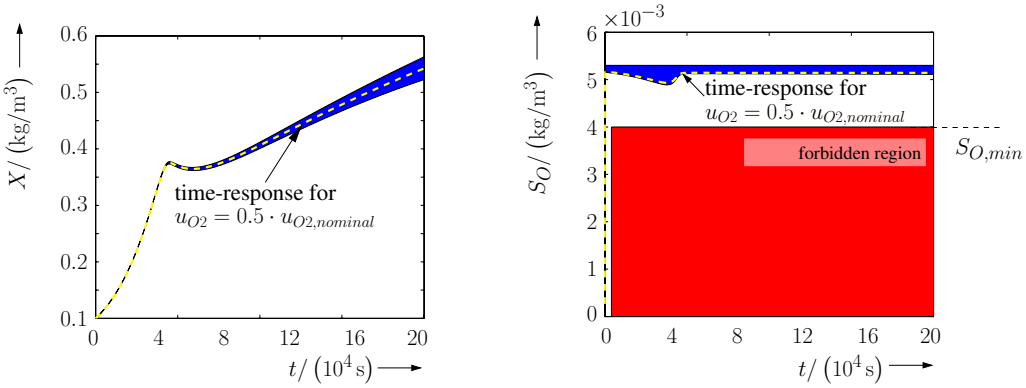

Figure 15. Bacteria concentration X and concentration S_O of dissolved oxygen.

centration S of organic substrate, the concentration X of bacteria, and the concentration S_O of dissolved oxygen in the aeration tank as well as the bacteria concentration X_{Set} in the settler.

With the prescribed bounds

$$\begin{aligned} \text{substrate:} &\begin{cases} S \text{ unbounded for} & t < 40,000\,\mathrm{s} \\ S \le S_{max} \text{ for} & t \ge 40,000\,\mathrm{s} \end{cases} \\ \text{oxygen:} &\begin{cases} S_O \text{ unbounded for} & t < 400\,\mathrm{s} \\ S_O \ge S_{O,min} \text{ for} & t \ge 400\,\mathrm{s} \end{cases} \end{aligned} \tag{35}$$

as robustness requirements, the computed validated state enclosures show that oxygen input rates from the interval $u_{O2} = [0.5\ ;\ 1.0] \cdot u_{O2,nominal}$ can be chosen without violation of the given bounds (35). Thus, the optimal choice of a constant oxygen input rate w.r.t. minimization of the operating costs is $u_{O2} = 0.5 \cdot u_{O2,nominal}$, see Figs. 14 and 15.

Note that this numerical proof of admissibility of control strategies for reliable plant operation using validated ODE solvers can be carried out analogously for control laws with time-varying oxygen input rates and for investigating parameter uncertainties. For details see [17].

6 State and Parameter Estimation Using Interval Observers

The applications which have been described in the previous Sections of this paper either dealt with estimation of system parameters in steady state or with the dynamical simulation of discrete-time and continuous-time systems without including any measured data. In the following, the concept of an interval observer [9] is discussed which relies on state-space representations of discrete-time systems as in eq. (1) and continuous-time systems as in eq. (2).

In addition to the system dynamics, mathematical models of the measurement process are necessary. They are

given by

$$y_{k+1} = h_{k+1}\left(x_{k+1}, p_{k+1}, \delta_{k+1}, u_{k+1}, k+1\right) \tag{36}$$

and

$$y\left(t_{k+1}\right) = h\left(x\left(t\right), p\left(t\right), \delta\left(t\right), u\left(t\right), t\right)\Big|_{t=t_{k+1}} \tag{37}$$

for discrete-time and continuous-time processes, respectively. In both cases, it is assumed that new measured data only become available at discrete points of time. For the sake of simplicity, the vector p of parameter uncertainties is now redefined such that it consists of the parameters of both the dynamical system model and the measurement model. Using the measurement equations (36) and (37), a model-based reconstruction of the state vector x as well as the parameter vector p is performed under consideration of the bounded measurement uncertainties $\delta \in [\delta] := \left[\underline{\delta}\,;\,\overline{\delta}\right]$.

The block diagram of the interval observer in Fig. 16 shows the two basic steps of state estimation. In the *prediction step*, propagation of all uncertainties is performed with the help of the mathematical model of the system dynamics until the point of time at which measured data are available. Then, the *correction step* eliminates those parts of the state enclosures (obtained by the prediction) which are inconsistent with the model of the measurement process under consideration of its uncertainties.

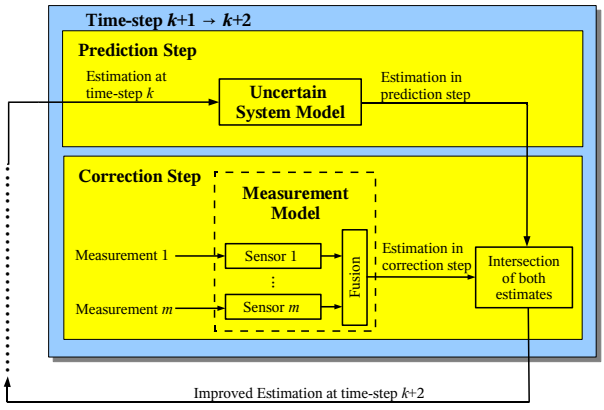

Figure 16. Interval observer.

In the following applications, state and parameter estimates computed by the interval observer are presented.

6.1 Electrostatic Micro Actuator

First, the electrostatic micro actuator in Fig. 17 is considered. For this device, the not directly measured initial gap x_{20} between the two plates of the capacitor, the position

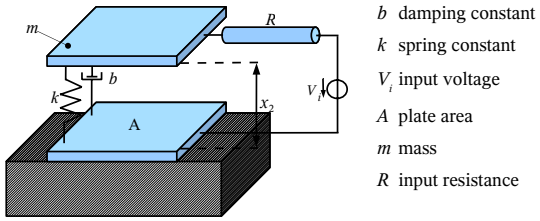

Figure 17. Electrostatic micro actuator.

$x_2\left(t\right)$, and the velocity $\dot{x}_2\left(t\right)$ have to be estimated. The dynamical system model is given by the ODEs [20]

$$\begin{aligned}
\dot{x}_1 &= \frac{1}{R}\left(V_i - \frac{x_1 x_2}{\epsilon A}\right) \\
\dot{x}_2 &= x_3 \\
\dot{x}_3 &= \frac{-1}{m}\left(\frac{x_1^2}{2\epsilon A} + k(x_2 - x_{20}) + b x_3\right)
\end{aligned} \tag{38}$$

with the uncertain initial conditions

$$x(0) \in \begin{bmatrix}[x_{10}] \\ [x_{20}] \\ [x_{30}]\end{bmatrix} = \begin{bmatrix}[0;0] \\ [0.9;1.1] \\ [0;0]\end{bmatrix} \tag{39}$$

and the time-invariant uncertain spring constant $k \in [0.8;1.2]$. Using the measurement equations

$$y_1 = \frac{x_1 x_2}{\epsilon A} + \delta_1 \quad \text{and} \quad y_2 = \frac{x_2}{\epsilon A} + \delta_2 \tag{40}$$

with the uncertainties $\delta_1 \in [-3;3]\cdot 10^{-4}$ and $\delta_2 \in [-1;1]\cdot 10^{-4}$, the estimates in Fig. 18 are obtained. A significant reduction of the initial uncertainty $[x_{20}]$ by the model-based state and parameter estimation approach is obvious.

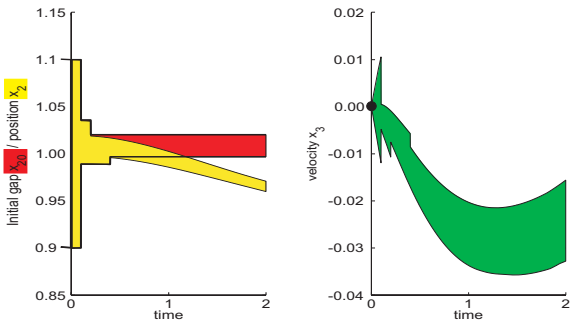

Figure 18. Estimates of position and velocity of the electrostatic micro actuator.

6.2 Micropositioning System

As a second application for the interval observer, the micropositioning system shown in Fig. 19 is discussed.

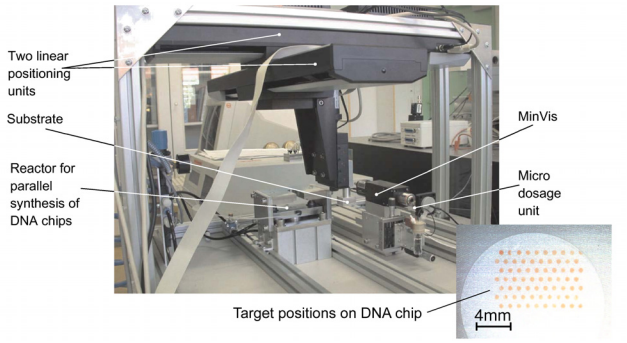

Figure 19. Micropositioning system.

Here, the task is the guaranteed positioning of microdrops on a DNA chip within given tolerances. For that purpose, the positioning unit is described by dynamical second order models in each axis. The dominating uncertainties in this system are the static friction coefficient F_s as well as the sliding friction coefficient μ which are depicted in the friction characteristic in Fig. 20.

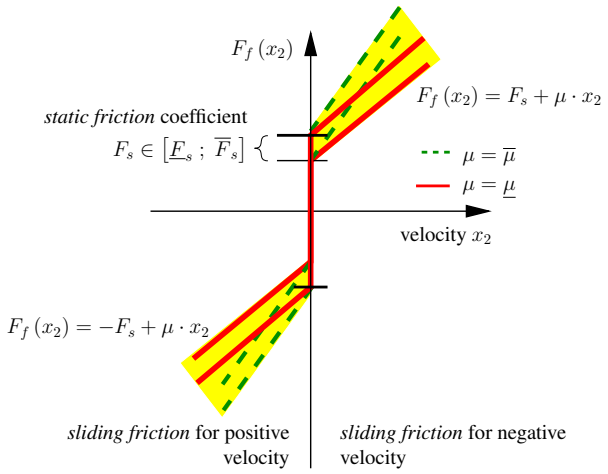

Figure 20. Friction characteristic.

The algorithm which is used for model-based estimation of both position and velocity of the positioning unit relies on validated integration of the dynamical system model in the prediction step. Here, all points of time have to be detected at which switchings between sliding and static friction occur. The exact procedure using a state transition diagram which is evaluated for all interval uncertainties has been published in [18].

In Fig. 21, results for two different cases are illustrated:
(i) The black solid lines show the influence of the parameter uncertainties in the friction characteristic in terms of worst-case bounds of the system's position.
(ii) Additionally, uncertain measurement information of the position is considered (marked by black dots). Then, compared to case (i), the bounds of the position estimate can be reduced significantly.

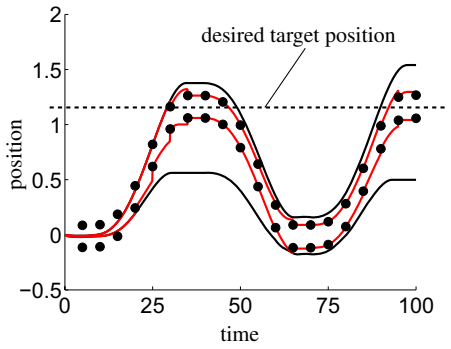

Figure 21. Position estimates.

7 Conclusions

The applications presented in this paper have been chosen to demonstrate how interval arithmetic evaluation methods for steady state analysis as well as simulation of both discrete-time and continuous-time systems can be applied successfully in engineering. The common goal of all applications has been to compute guaranteed enclosures of all physically relevant states and parameters. Besides simulation of the dynamical system behavior in open-loop and closed-loop operation, the design of a model-based interval observer for guaranteed state and parameter estimation has been described. In this approach, measurement information can be used efficiently to eliminate parts of the state enclosures which are inconsistent either with the mathematical model of the system dynamics or with the model of the measurement process.

As shown in this contribution, the most important property of interval algorithms, namely the ability to compute guaranteed enclosures [7], is especially relevant in the analysis and the design of technical and non-technical systems. Based on mathematical system models, the worst-case influence of uncertainties as well as the robustness, reliability, cost-effectiveness, and safety of a system can be investigated by computation of guaranteed bounds of the corresponding system states.

In order to apply interval algorithms to a wider class of problems, further general implementations have to be made

available. Additionally, future research aiming at the development of improved and novel interval arithmetic tools has to consider the necessity to deal with uncertain dynamical systems which include discontinuities and model switchings in the systems' representations, e.g. hystereses in electro-mechanical applications. Finally, the development of interval arithmetic methods for the computation of robust and optimal control strategies [11, 16] for high-dimensional nonlinear systems with non-negligible influence of uncertainties will be an important field for future developments.

Future research will be directed towards both establishing interval techniques in the computing mainstream by further developing software tools and — most important — demonstrating successful applications.

References

[1] E. Auer, A. Rauh, E. P. Hofer, and W. Luther. Validated Modeling of Mechanical Systems with SMARTMOBILE: Improvement of Performance by VALENCIA-IVP. In *Proc. of Dagstuhl Seminar 06021: Reliable Implementation of Real Number Algorithms: Theory and Practice*, Lecture Notes in Computer Science, 2006. In print.

[2] J. M. Hammersley and D. C. Handscomb. *Monte-Carlo Methods*. John Wiley & Sons, New York, 1964.

[3] E. Hansen. *Global Optimization Using Interval Analysis*. Marcel Dekker, New York, 1992.

[4] J. Heeks. *Charakterisierung unsicherer Systeme mit intervallarithmetischen Methoden*. PhD thesis, Universität Ulm, Abteilung Mess-, Regel- und Mikrotechnik, 2002.

[5] J. Heeks, E. P. Hofer, B. Tibken, K. Lunde, and K. Thorwart. Simulation of a Controlled Aircraft Elevator Under Sensor Uncertainties. In W. Krämer and J. W. von Gudenberg, editors, *Scientific Computing, Validated Numerics, Internal Methods*, Kluwer Academic/Plenum Publishers, New York, pages 227–237. 2001.

[6] E. P. Hofer, B. Tibken, and C. Rembe. Guaranteed Parameter Estimation for Characterization of Microdevices. In E. Reithmeier and G. Leitmann, editors, *Proc. of 10th Workshop on Dynamics and Control, Lambrecht, Germany, 1998*, Complex Dynamical Systems with Incomplete Information, pages 81–93. Shaker Verlag, Aachen, 1999.

[7] E. P. Hofer, B. Tibken, and M. Vlach. Traditional Parameter Estimation Versus Estimation of Guaranteed Parameter Sets. In W. Krämer and J. W. von Gudenberg, editors, *Scientific Computing, Validated Numerics, Internal Methods*, Kluwer Academic/Plenum Publishers, New York, pages 241–253. 2001.

[8] L. Jaulin, M. Kieffer, O. Didrit, and É. Walter. *Applied Interval Analysis*. Springer, London, 2001.

[9] M. Kletting, A. Rauh, H. Aschemann, and E. P. Hofer. Interval Observer Design for Nonlinear Systems with Uncertain Time-Varying Parameters. In *Proc. of 12th IEEE Intl. Conference on Methods and Models in Automation and Robotics MMAR*, pages 361–366, Miedzyzdroje, Poland, 2006.

[10] M. Kletting, A. Rauh, H. Aschemann, and E. P. Hofer. Consistency Tests in Guaranteed Simulation of Nonlinear Uncertain Systems with Application to an Activated Sludge Process. *Journal of Computational and Applied Mathematics*, 199(2):213–219, 2007.

[11] Y. Lin and M. A. Stadtherr. Deterministic Global Optimization for Dynamic Systems Using Interval Analysis. In *Book of Abstracts of 12th GAMM-IMACS Intl. Symposium on Scientific Computing, Computer Arithmetic, and Validated Numerics SCAN 2006*, page 74, Duisburg, Germany, 2006.

[12] K. Makino. *Rigorous Analysis of Nonlinear Motion in Particle Accelerators*. PhD thesis, Michigan State University, 1998.

[13] R. Moore. *Methods and Applications of Interval Analysis*. SIAM, Philadelphia, 1979.

[14] N. S. Nedialkov. *Computing Rigorous Bounds on the Solution of an Initial Value Problem for an Ordinary Differential Equation*. PhD thesis, Graduate Department of Computer Science, University of Toronto, 1999.

[15] N. S. Nedialkov, K. R. Jackson, and J. D. Pryce. An Effective High-Order Interval Method for Validating Existence and Uniqueness of the Solution of an IVP for an ODE. *Reliable Computing*, 7:449–465, 2001.

[16] A. Rauh and E. P. Hofer. Interval Arithmetic Optimization Techniques for Uncertain Discrete-Time Systems. In E. P. Hofer and E. Reithmeier, editors, *Proc. of 13th Int. Workshop on Dynamics and Control, Wiesensteig, Germany, 2005*, Modeling and Control of Autonomous Decision Support Based Systems, pages 141–148. Shaker Verlag, Aachen, 2005.

[17] A. Rauh, M. Kletting, H. Aschemann, and E. P. Hofer. Robust Controller Design for Bounded State and Control Variables and Uncertain Parameters Using Interval Methods. In *Proc. of 5th Intl. Conference on Control and Automation ICCA*, pages 777–782, Budapest, Hungary, 2005.

[18] A. Rauh, M. Kletting, H. Aschemann, and E. P. Hofer. Interval Methods for Simulation of Dynamical Systems with State-Dependent Switching Characteristics. In *Proc. of IEEE Intl. Conference on Control Applications CCA 2006*, pages 355 – 360, Munich, Germany, 2006.

[19] A. Rauh, M. Kletting, H. Aschemann, and E. P. Hofer. Reduction of Overestimation in Interval Arithmetic Simulation of Biological Wastewater Treatment Processes. *Journal of Computational and Applied Mathematics*, 199(2):207–212, 2007.

[20] A. Rauh, M. Kletting, and E. P. Hofer. Model-Based State and Parameter Estimation for Micro-Mechatronic Systems with Interval Bounded Uncertainties. In A. Weckenmann, editor, *CD-Proc. of 10th CIRP Intl. Conference on Computer Aided Tolerancing, Erlangen, Germany, 2007*, Reports from the Chair Quality Management and Manufacturing Metrology, QFM Report 16. Shaker Verlag, Aachen, 2007.

[21] B. Tibken, E. P. Hofer, J. Heeks, K. Thorwart, and H. Aschemann. Simulation of a Common Rail Fuel Injection System Using Interval Arithmetic. SCAN 2002. Paris, France, 2002.

[22] B. Tibken, E. P. Hofer, and W. Seibold. Quality Control of Valve Push Rods Using Interval Artihmetic. In *Proc. of 14th Triennial World Congress Intl. Federation of Automatic Control IFAC*, volume A, pages 409–412, Beijing, P. R. China, 1999.